

## Original Article

# $^{11}\text{C}$ -Pittsburgh compound B and $^{18}\text{F}$ -THK 5351 positron emission tomography brain imaging in cognitively normal individuals

**ABSTRACT**

Abnormal beta-amyloid plaques and tau protein accumulation are the core pathologic features of Alzheimer's disease. However, the accumulation of these proteins is also common in cognitively normal elderly people. Therefore, this study is aimed to evaluate the amyloid and tau accumulation in the cognitively normal population. A preliminary prospective study was conducted on 24 cognitively normal individuals who underwent Pittsburgh compound B ( $^{11}\text{C}$ -PiB) and  $^{18}\text{F}$ -THK 5351 positron emission tomography (PET)/computed tomography scans. The standardized uptake value ratio (SUVR) was used for quantitative analysis of the two tracers and comparisons between two age groups: 60 years and >60 years. Co-registration was applied between the dynamic acquisition PET and T1-weighted magnetic resonance imaging to delineate various cortical regions. P-mod software with the automated anatomical labeling-merged atlas was employed to generate automatic volumes of interest for different brain regions. The posterior cingulate versus precuneus SUVRs of PiB uptake was  $1.40 \pm 0.07$  and  $1.38 \pm 0.22$  versus  $1.17 \pm 0.07$  and  $1.14 \pm 0.18$  in those aged  $\leq 60$  years and >60 years, respectively, whereas the SUVRs of THK5351 retention at brain stem versus inferior temporal SUVRs were  $1.84 \pm 0.06$  and  $1.91 \pm 0.18$  versus  $1.37 \pm 0.04$  and  $1.48 \pm 0.21$  in the age groups of 60 years and >60 years, respectively ( $P = 0.20$ ). Our findings allow the determination of the preliminary optimal cutoff points for SUVRs in amyloid and tau PET studies. Ultimately, these values can be applied to normal databases in clinical use to improve quantitative analysis.

**Keywords:**  $^{11}\text{C}$ -Pittsburgh compound-B,  $^{18}\text{F}$ -THK 5351, Alzheimer's disease, cognitively normal individual, positron emission tomography

**INTRODUCTION**

It is undeniable that many countries are now confronted with aging societies. When dealing with global health-care problems, neurodegenerative disorders are the most common age-related diseases challenging the world's elderly population. In particular, the problem of dementia constitutes a health concern among the elderly, and better screening and prevention programs are needed. Alzheimer's disease (AD) is the most common cause of dementia. The pooled incidence proportion of dementia due to AD among individuals >60 years old is 34.1/1000 persons-years (confidence interval [CI] 95%: 16.4–70.9), and the incidence rate is 15.8/1000 person-years (CI 95%: 12.9–19.4).<sup>[1]</sup>

Noninvasive positron emission tomography (PET) brain imaging is a useful tool for supporting the quantitative

characterization of neurological conditions such as AD, as it allows determination of the functional use or accumulation of radiopharmaceuticals in specific brain regions.<sup>[2]</sup> AD is

**CHANISA CHOTIPANICH, ATTAPON JANTARATO, ANCHISA KUNAWUDHI, SUPAPORN KONGTHAI, CHETSADAPORN PROMTEANGTRONG**

National Cyclotron and PET Centre, Chulabhorn Hospital, Chulabhorn Royal Academy, Bangkok, Thailand


**Address for correspondence:** Prof. Chanisa Chotipanich, National Cyclotron and PET Centre, Chulabhorn Hospital, Chulabhorn Royal Academy, 906 Kamphaeng Phet 6 Road, Talat Bang Khen, Lak Si, Bangkok 10210, Thailand.  
E-mail: chanisa.cho@pccms.ac.th

**Submitted:** 21-Apr-2020, **Revised:** 29-Apr-2020, **Accepted:** 01-May-2020, **Published:** 27-Jun-2020

This is an open access journal, and articles are distributed under the terms of the Creative Commons Attribution-NonCommercial-ShareAlike 4.0 License, which allows others to remix, tweak, and build upon the work non-commercially, as long as appropriate credit is given and the new creations are licensed under the identical terms.

**For reprints contact:** WKHLRPMedknow\_reprints@wolterskluwer.com

**How to cite this article:** Chotipanich C, Jantarato A, Kunawudhi A, Kongthai S, Promteangtrong C.  $^{11}\text{C}$ -Pittsburgh compound B and  $^{18}\text{F}$ -THK 5351 positron emission tomography brain imaging in cognitively normal individuals. World J Nucl Med 2021;20:133-8.

Access this article online	
<b>Website:</b> www.wjnm.org	<b>Quick Response Code</b> 
<b>DOI:</b> 10.4103/wjnm.WJNM_57_20	

characterized by the deposition of both amyloid protein and tau protein in the brain.<sup>[3]</sup> Thus, amyloid and tau protein PET scans are needed to confirm the diagnosis in indeterminate or atypical cases, and especially to aid in the early detection of AD in subjects with mild cognitive impairment (MCI).<sup>[3,4]</sup>

Positron emission tomography/computed tomography (PET/CT) scanning with Pittsburgh compound B (<sup>11</sup>C-PiB) and <sup>18</sup>F-THK 5351 allows both visual (imaging) and quantitative analysis by standardized uptake value ratio (SUVR) of amyloid- $\beta$  plaques and Tau protein aggregations in the brain, which is clinically beneficial and important for the diagnosis of early-stage and preclinical stage AD, as well as for the differentiation of AD from other neurodegenerative diseases.<sup>[4,5]</sup>

For quantitative analysis using PET, the SUVR plays a significant role as an important parameter for PET neuroimaging diagnosis. Visual analysis may not provide adequate information for accurate diagnosis because of biased judgments related to contrast adjustment or even the physician's experience, which may prevent the clear determination of physiological uptake.<sup>[6]</sup>

However, the quantitative assessment of amyloid plaques and tau protein using PET requires consistent effort to standardize the protocols. The steps involve proper subject selection and management, administration of calibrated radiotracer dosage, image analysis and quality control, identification of brain reference regions, and optimization of various image processing and segmentation methods.<sup>[7]</sup>

In addition to the technical aspects and study setting, the biological condition of the population should also be considered. It has been demonstrated that differences in the morphology of the skulls of different ethnicities contribute to different brain shapes and volumes that affect the accumulation of amyloid and tangles,<sup>[8]</sup> associated with different SUVR cutoffs between different normal populations.<sup>[7]</sup>

In this study, we measured local SUVRs in cognitively normal elderly people to establish reliable SUVR thresholds for diagnosing Alzheimer's disease in our population, and to thereby improve the efficacy of patient management.

## MATERIALS AND METHODS

This study was approved by the Human Research Ethics Committee of our institute on August 17, 2016. Project code was 023/2559. Before the study, written informed consent

was obtained from all participants for participation in the study of data for research and educational purposes.

### Participants

Twenty-four individuals (13 men, 11 women; aged: 42–79 years; mean age:  $59.67 \pm 10.84$  years) who were diagnosed as cognitively normal on examinations by neurologists and neuro-psychiatrists participated in this study. Cognitively normal criteria were defined as (1) mini-mental state examination (MMSE) or 24 of higher or a score of  $>25$  on the Montreal Cognitive Assessment (MoCA), (2) Clinical Dementia Rating of 0, (3) preserved activities of daily living, (4) absence of significant levels of impairment in other cognitive domains, (5) no sign and symptom of MCI or dementia, and (6) not diagnosed with probable AD by using criteria from the National Institute on Aging-Alzheimer's Association workgroups.<sup>[9]</sup> All subjects had no concurrent underlying disease such as hypertension, dyslipidemia, diabetes Mellitus, cardiovascular disease, pulmonary or renal condition. No participants had a history of psychological or neurological diseases, use of psychotropic drugs, or cancer found within the past 5 years. Magnetic resonance imaging (MRI) was performed in all participants. The participants were separated into two age groups:  $\leq 60$  years and  $>60$  years.

MRI brain of each cognitively normal individuals showed no focal mass, acute infarction, intracranial hemorrhage, hydrocephalus, extra-axial collection, or brain herniation.

### Procedures

All participants underwent amyloid PET with <sup>11</sup>C-PiB and tau PET with <sup>18</sup>F-THK 5351, using a Siemens Biograph 16 scanner in three-dimensional (3D) mode. For each patient, both scans were performed within 2 weeks.

#### <sup>11</sup>C-Pittsburgh compound B imaging procedure

All participants were scanned using dynamic imaging started immediately after intravenous injection of 555 MBq (15 mCi) of <sup>11</sup>C-PiB. Dynamic brain PET scanning was obtained for 70 min, and brain CT images were acquired for attenuation correction. The image acquisition parameters included matrix size =  $168 \times 168$ , zoom = 1, and Gaussian filtering with a full-width at half-maximum (FWHM) of 5.0. Image reconstruction was performed in 7 frames of 10 min per frame, using ordered subset expectation maximization (OSEM) with 4 iterations, 8 subsets, and 4-mm pixel size. The iteratively reconstructed images acquired from 50 to 70 min were used for the quantitative analysis.

#### <sup>18</sup>F-THK 5351 imaging procedure

Dynamic imaging was performed immediately after intravenous injection of 185 MBq (5 mCi) of <sup>18</sup>F-THK 5351.

Dynamic brain PET scanning was obtained for 90 min and brain CT images were acquired for attenuation correction. The image acquisition parameters included matrix size =  $168 \times 168$ , zoom = 1, and Gaussian filtering with an FWHM of 5.0. Image reconstruction was performed in 4 frames of 20 min per frame, using OSEM with 4 iterations, 8 subsets, and 4-mm pixel size. The iteratively reconstructed images acquired from 40 to 60 min were used for quantitative analysis.

### Magnetic resonance imaging acquisition

T1-weighted MRI (T1MRI) was acquired for all participants using a 3.0-T MRI Siemens Trio scanner. The parameters for the 3D T1MRI included: Sagittal slice thickness of 1.0 mm; over contiguous slices with 50% overlap; repetition time of 1600 ms; echo time of 2.03 ms; flip angle of  $9^\circ$ ; field of view of  $240 \text{ mm} \times 240 \text{ mm}$ ; and a matrix size of  $256 \times 256$  pixels reconstructed to  $480 \times 480$ .

T1MRI was used for registration and delineation of the brain reference regions using the PMOD Neuro tool (PMOD Technologies, Zürich, Switzerland).

### Data and statistical analysis

Data processing and analysis of the PET imaging was conducted using P-mod Neuro tool (PMOD Technologies, Switzerland), as shown in Figure 1. Both the  $^{11}\text{C}$ -PiB and  $^{18}\text{F}$ -THK 5351 PET images were automatically co-registered within each individual, using an automatic voxel of interest (VOI) method. The PET images were then registered to the T1MRI from each subject. The T1MRI images were used for the registration and delineation of the brain reference regions, with the data being standardized to the Montreal Neurological Institute T1MRI template atlas. VOIs were automatically outlined on the normalized MRI according to maximum probability following the Automated Anatomical Labeling - merged atlas. Then, the SUVRs of  $^{11}\text{C}$ -PiB and  $^{18}\text{F}$ -THK 5351 were measured for various cortical regions, using the cerebellar grey matter as a reference region. Eight regions were measured for  $^{11}\text{C}$ -PiB, with these being the orbitofrontal, precuneus, parietal, anterior cingulate, posterior cingulate, superior parietal, lateral temporal, and occipital areas. The regions measured for  $^{18}\text{F}$ -THK 5351 consisted of the anterior cingulate, brain stem, caudate nucleus, white matter, entorhinal cortex, frontal cortex, fusiform gyrus, hippocampus, inferior temporal cortex, lingual gyrus, middle temporal gyrus, occipital cortex, pallidum, parahippocampal gyrus, parietal cortex, posterior cingulate, precuneus, putamen, and thalamus.

Analysis of variance and multiple unpaired *t*-test and one-sample *t*-tests were performed to compare tracer uptake across the various cortical regions. One sample *t*-test was

also performed between our SUVR in specific regions and reviewed SUVR from previous studies. A value of  $P < 0.05$  was considered statistically significant, and all statistical analyses were performed using STATA software version 11 (StataCorp LLC, Texas, USA).

## RESULTS

The participants' characteristics and details are shown in Tables 1 and 2.

### Quantitative analysis of $^{11}\text{C}$ -Pittsburgh compound B

The participants aged  $\leq 60$  years showed the highest cortical uptake of  $^{11}\text{C}$ -PiB in the posterior cingulate gyrus, with average SUVRs of  $1.40 \pm 0.07$ , followed by  $1.31 \pm 0.08$  in the anterior cingulate gyrus. The other regions, including the orbitofrontal, precuneus, parietal, lateral temporal, and occipital areas, demonstrated SUVRs close to 1.12–1.20.

Similarly, in the age group  $> 60$  years, the posterior cingulate also yielded the highest SUVR of  $1.38 \pm 0.22$ , followed by  $1.29 \pm 0.17$  in the anterior cingulate gyrus. However, there was no statistically significant difference in cortical uptake between the two age groups [Table 3].

### Quantitative analysis of $^{18}\text{F}$ -THK 5351

The  $\leq 60$  years age group showed the highest retention of  $^{18}\text{F}$ -THK 5351 in the pallidum, with an average SUVR of  $2.49 \pm 0.15$ , with high average SUVRs of  $> 2.00$  also being found in three other regions, the hippocampus ( $2.01 \pm 0.11$ ),

**Table 1: Participants' characteristics**

Characteristics	
Sex (count, %)	
Male	13 (54)
Female	11 (46)
MoCA (score)	
Range	25-30
Mean	$27.29 \pm 1.57$
Median	27.5
Age $\leq 60$ (year)	
<i>n</i>	13
Range	42-60
Mean	$51.38 \pm 5.56$
Age $> 60$ (year)	
<i>n</i>	11
Range	61-79
Mean	$69.45 \pm 6.1$
Education, (year)	
Range	4-20
Mean	$14.8 \pm 4.2$
Median	16

MOCA: Montreal cognitive assessment

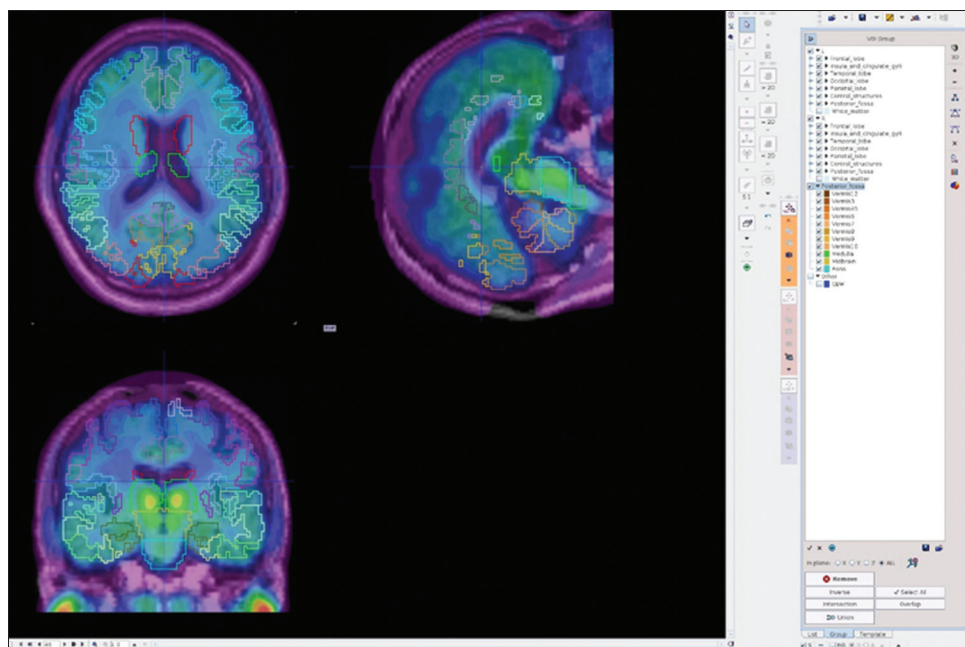


**Figure 1:** Data processing and analysis of positron emission tomography imaging was conducted using the P-mod Neuro tool. The data were analyzed and processed following the automatic software processing, which include denoising, normalization, reorientation of positron emission tomography data and segmentation of magnetic resonance imaging. The final step is the fusion positron emission tomography and magnetic resonance imaging with the automatic segmentation according to the automated anatomical labelling-merged atlas

putamen ( $2.09 \pm 0.08$ ), and thalamus ( $2.11 \pm 0.11$ ). The SUVRs of the inferior temporal cortex and brain stem were  $1.37 \pm 0.04$  and  $1.84 \pm 0.06$ , respectively.

Similarly,  $^{18}\text{F}$ -THK binding in the age group  $>60$  years showed the highest SUVR of  $3.01 \pm 0.55$  in the pallidum, followed by high values over 2.00 in the same areas as in the group aged  $\leq 60$  years, including the hippocampus ( $2.14 \pm 0.22$ ), putamen ( $2.33 \pm 0.39$ ), and thalamus ( $2.26 \pm 0.28$ ). The SUVRs of the inferior temporal cortex and brain stem were  $1.48 \pm 0.21$  and  $1.91 \pm 0.18$ , respectively. There was a statistically significant difference in the SUVRs of the entorhinal cortex, pallidum, and putamen between the two age groups [ $P < 0.05$ ; Table 4].

**DISCUSSION**

Amyloid plaque normally accumulates in the human brain with or without AD pathology. Hence, the retention of amyloid can be observed in normal brain regions, but in different degrees depending on age, apolipoprotein E (APOE) genotype, and gender.<sup>[10]</sup> Moreover, the PiB accumulation pattern in healthy control participants described by Cohen *et al.* showed little or no accumulation in cortical brain regions.<sup>[11]</sup> This indicates that 10%–30% of normal elderly participants could show significant PiB retention.<sup>[10]</sup>

In our study, the highest cortical uptake of PiB occurred in the anterior and posterior cingulate gyrus. In accord with this,

**Table 2: Participants’ details**

Subjects	Sex	Age	MoCA score
<b>Age group <math>\leq 60</math> years</b>			
PT01	Female	42	28
PT02	Male	44	27
PT03	Female	46	28
PT04	Female	49	26
PT05	Male	50	30
PT06	Male	50	29
PT07	Female	51	29
PT08	Female	51	28
PT09	Male	53	29
PT10	Female	54	26
PT11	Female	58	26
PT12	Female	60	26
PT13	Male	60	27
<b>Age group <math>&gt;60</math> years</b>			
PT14	Male	61	26
PT15	Female	63	26
PT16	Male	64	25
PT17	Female	67	27
PT18	Male	67	29
PT19	Female	67	26
PT20	Male	70	30
PT21	Male	72	29
PT22	Male	77	25
PT23	Male	77	30
PT24	Male	79	25

MOCA: Montreal cognitive assessment

Wakabayashi *et al.*<sup>[12]</sup> reported the highest cortical uptake of PiB in the posterior cingulate, with an SUVR of 1.25 in the

**Table 3: Mean standardized uptake value ratio on <sup>11</sup>C-PiB positron emission tomography imaging**

Region of interest	Age ≤60 years (n=13)	Age >60 years (n=11)	P
Orbitofrontal	1.20±0.11	1.25±0.13	0.41
Precuneus	1.17±0.07	1.14±0.18	0.62
Parietal	1.14±0.08	1.08±0.18	0.28
Anterior cingulate	1.31±0.08	1.29±0.17	0.67
Posterior cingulate	1.40±0.07	1.38±0.22	0.69
Superior parietal	1.06±0.11	0.96±0.18	0.11
Lateral temporal	1.12±0.07	1.11±0.09	0.70
Occipital	1.16±0.09	1.14±0.12	0.67

**Table 4: Mean standardized uptake value ratio on <sup>18</sup>F-THK 5351 imaging**

Region of interest	Age ≤60 years (n=13)	Age >60 years (n=11)	P
Anterior cingulate	1.67±0.05	1.71±0.19	0.43
Brain stem	1.84±0.06	1.91±0.18	0.20
Caudate nucleus	1.98±0.18	1.93±0.27	0.58
White matter	1.40±0.08	1.48±0.18	0.14
Entorhinal cortex	1.51±0.08	1.69±0.24	0.02
Frontal cortex	1.25±0.04	1.28±0.13	0.51
Fusiform gyrus	1.40±0.05	1.48±0.20	0.17
Hippocampus	2.01±0.11	2.14±0.22	0.08
Inferior temporal cortex	1.37±0.04	1.48±0.21	0.09
Lingual gyrus	1.20±0.06	1.22±0.14	0.69
Middle temporal gyrus	1.27±0.04	1.34±0.16	0.15
Occipital cortex	1.16±0.05	1.18±0.12	0.56
Pallidum	2.49±0.15	3.01±0.55	0.00
Parahippocampal gyrus	1.78±0.09	1.90±0.23	0.11
Parietal cortex	1.16±0.05	1.18±0.11	0.68
Posterior cingulate	1.45±0.06	1.49±0.15	0.39
Precuneus	1.26±0.03	1.26±0.11	0.89
Putamen	2.09±0.08	2.33±0.39	0.02
Thalamus	2.11±0.11	2.26±0.28	0.10

PiB negative group who aged  $66.5 \pm 7.0$  years. Our study showed the highest PiB uptake in the same brain region, and there was a significant difference ( $P < 0.05$ ) in the SUVRs of the posterior cingulate gyrus between two studies. Thus, there were still some SUVR differences between both studies, despite them being from the same Asian population. The results of our study are not directly comparable with those of Ismail *et al.*<sup>[13]</sup> and Villeneuve *et al.*<sup>[14]</sup> who employed a global cortical SUVR measure combining multiple brain regions, as we evaluated the average cortical SUVR for each region, including the region of PiB accumulation.

Our findings regarding <sup>18</sup>F-THK 5351 accumulation were similar to that of Okamura *et al.*,<sup>[15]</sup> who showed high uptake in the pallidum and thalamus regions due to monoamine oxidase (MAO) binding, with these regions being considered as off-target binding brain regions for THK 5351. Our results

were also consistent with those of Lockhart *et al.*<sup>[16]</sup> who reported high SUVRs in the pallidum and thalamus regions. THK compounds also show off-target binding to monoamine oxidase B (MAO-B), resulting in uptake at midbrain and basal ganglia. Although the affinity between MAO-B and <sup>18</sup>F-THK-5351 should not affect the signal observed by PET,<sup>[17]</sup> <sup>18</sup>F-THK 5351 PET/CT should be carefully interpreted. We also found a statistically significant difference in the THK 5351 SUVRs of the entorhinal cortex, pallidum, and putamen between the two age groups, further study in a large number of participants is needed for clarification.

In the inferior temporal region, an area of particular interest for preclinical Alzheimer's diagnosis, Kikuchi *et al.*<sup>[18]</sup> and Harada *et al.*<sup>[19]</sup> described THK 5351 SUVRs of  $1.56 \pm 0.09$  in the right middle inferior temporal region,  $1.52 \pm 0.12$  in the left middle inferior temporal region, and a range of 1.44–1.67 in the inferior temporal lobe. In comparison, we found SUVRs of  $1.37 \pm 0.04$  and  $1.48 \pm 0.21$  for the age groups of  $\leq 60$  years and  $> 60$  years, respectively, without statistically significant difference. Even though these values are all from reports studying Asian populations, there was a statistically significant difference in the SUVRs in this region between the earlier studies and ours ( $P < 0.05$  in one sample *t*-test analysis).

Finally, we found statistically significant SUVR differences between our study and previous studies for both amyloid and Tau. Thus, SUVRs from populations with different ethnicities should not be used as reference values, as there may be numerous factors influencing variation, such as the biological factors reported by Duara *et al.*,<sup>[20]</sup> who described variation in SUVR thresholds for amyloid retention resulting from ethnicity (Hispanic or nonHispanic), age, sex, cognitive status, and APOE  $\epsilon 4$  carrier status. Moreover, physical factors such as brain volume, technical aspects such as the difference of PET/CT machine's performance efficiency, data acquisition parameter setting, and the diversity of quantitative methods used for the analysis should also be considered.

Our study was limited by the small number of participants, which might have decreased the statistical power for the discrimination of differences between the two age groups. In particular, our study reports only preliminary findings, and further study with larger sample size is recommended to confirm our findings.

## CONCLUSION

Our study demonstrates the preliminary normal SUVR database for <sup>11</sup>C-PiB and <sup>18</sup>F-THK 5351 PET/CT. Nonetheless,

the local cut-off points for SUVR database values should be carefully ratified in clinical practice and research, to ensure better accuracy, quantitative analysis improvement, and precision in preclinical AD evaluation. As well, normal SUVR database values should also be recommended as a model for reliable thresholds in different ethnicities towards better diagnosis and management efficacy of Alzheimer's disease patients.

### Financial support and sponsorship

Chulabhorn Hospital, Chulabhorn Royal Academy.

### Conflicts of interest

There are no conflicts of interest.

### REFERENCES

1. Fiest KM, Roberts JI, Maxwell CJ, Hogan DB, Smith EE, Frolkis A, *et al.* The prevalence and incidence of dementia due to Alzheimer's disease: A systematic review and meta-analysis. *Can J Neurol Sci* 2016;43 Suppl 1:S51-82.
2. Zhu L, Ploessl K, Kung HF. PET/SPECT imaging agents for neurodegenerative diseases. *Chem Soc Rev* 2014;43:6683-91.
3. Higashi T, Nishii R, Kagawa S, Kishibe Y, Takahashi M, Okina T, *et al.* 18 F-FPYBF-2, a new F-18-labelled amyloid imaging PET tracer: First experience in 61 volunteers and 55 patients with dementia. *Ann Nucl Med* 2018;32:206-16.
4. Leuzy A, Chiotis K, Lemoine L, Gillberg PG, Almkvist O, Rodriguez-Vieitez E, *et al.* Tau PET imaging in neurodegenerative tauopathies-still a challenge. *Mol Psychiatry* 2019;24:1112-34.
5. Su Y, D'Angelo GM, Vlassenko AG, Zhou G, Snyder AZ, Marcus DS, *et al.* Quantitative analysis of PiB-PET with FreeSurfer ROIs. *PLoS One* 2013;8:e73377.
6. Mountz JM, Laymon CM, Cohen AD, Zhang Z, Price JC, Boudhar S, *et al.* Comparison of qualitative and quantitative imaging characteristics of [11C]PiB and [18F]flutemetamol in normal control and Alzheimer's subjects. *NeuroImage Clin* 2015;9:592-8.
7. Schmidt ME, Chiao P, Klein G, Matthews D, Thurfjell L, Cole PE, *et al.* The influence of biological and technical factors on quantitative analysis of amyloid PET: Points to consider and recommendations for controlling variability in longitudinal data. *Alzheimers Dement* 2015;11:1050-68.
8. Kasai K, Iwanami A, Yamasue H, Kuroki N, Nakagome K, Fukuda M. Neuroanatomy and neurophysiology in schizophrenia. *Neurosci Res* 2002;43:93-110.
9. McKhann GM, Knopman DS, Chertkow H, Hyman BT, Jack CR Jr., Kawas CH. The diagnosis of dementia due to Alzheimer's disease: Recommendations from the National Institute on Aging-Alzheimer's Association workgroups on diagnostic guidelines for Alzheimer's disease. *Alzheimers Dement* 2011;7:263-9.
10. Scheinin NM, Wikman K, Jula A, Perola M, Vahlberg T, Rokka J, *et al.* Cortical <sup>11</sup>C-PiB uptake is associated with age, APOE genotype, and gender in "healthy aging". *J Alzheimers Dis* 2014;41:193-202.
11. Cohen AD, Rabinovici GD, Mathis CA, Jagust WJ, Klunk WE, Ikonovic MD. Using Pittsburgh compound B for *in vivo* PET imaging of fibrillar amyloid-beta. *Adv Pharmacol* 2012;64:27-81.
12. Wakabayashi Y, Ishii K, Hosokawa C, Hyodo T, Kaida H, Yamada M, *et al.* Increased Pittsburgh compound-B accumulation in the subcortical white matter of Alzheimer's disease brain. *Kobe J Med Sci* 2017;62:E136-41.
13. Ismail R, Parbo P, Hansen KV, Schaldemose JL, Dalby RB, Tietze A, *et al.* Abnormal amyloid load in mild cognitive impairment: The effect of reducing the PiB-PET Threshold. *J Neuroimaging* 2019;29:499-505.
14. Villeneuve S, Rabinovici GD, Cohn-Sheehy BI, Madison C, Ayakta N, Ghosh PM, *et al.* Existing Pittsburgh compound-B positron emission tomography thresholds are too high: Statistical and pathological evaluation. *Brain* 2015;138:2020-33.
15. Okamura N, Harada R, Ishiki A, Kikuchi A, Nakamura T, Kudo Y. The development and validation of tau PET tracers: Current status and future directions. *Clin Transl Imaging* 2018;6:305-16.
16. Lockhart SN, Baker SL, Okamura N, Furukawa K, Ishiki A, Furumoto S, *et al.* Dynamic PET measures of tau accumulation in cognitively normal older adults and Alzheimer's disease patients measured using [18F] THK-5351. *PLoS One* 2016;11:e0158460.
17. Lemoine L, Gillberg PG, Svedberg M, Stepanov V, Jia Z, Huang J, *et al.* Comparative binding properties of the tau PET tracers THK5117, THK5351, PBB3, and T807 in postmortem Alzheimer brains. *Alzheimers Res Ther* 2017;9:96.
18. Kikuchi A, Okamura N, Hasegawa T, Harada R, Watanuki S, Funaki Y, *et al.* *In vivo* visualization of tau deposits in corticobasal syndrome by 18F-THK5351 PET. *Neurology* 2016;87:2309-16.
19. Harada R, Okamura N, Furumoto S, Furukawa K, Ishiki A, Tomita N, *et al.* 18F-THK5351: A Novel PET radiotracer for imaging neurofibrillary pathology in Alzheimer disease. *J Nucl Med* 2016;57:208-14.
20. Duara R, Loewenstein DA, Lizaraga G, Adjouadi M, Barker WW, Greig-Custo MT, *et al.* Effect of age, ethnicity, sex, cognitive status and APOE genotype on amyloid load and the threshold for amyloid positivity. *Neuroimage Clin* 2019;22:101800. doi: 10.1016/j.nicl.2019.101800.